GRAIN REFINING AND SUPERPLASTIC FORMING OF ALUMINUM ALLOY 6013

Y.H. Chung, L.P. Troeger, and E.A. Starke, Jr.
Department of Materials Science and Engineering, University of Virginia, Thornton Hall,
Charlottesville, VA 22903, U.S.A.

Abstract

A fine grain structure is an essential requirement for superplastic forming of aluminum alloys. Fine grain structures may be obtained in aluminum alloy 6013 by thermo-mechanical processing and dynamic recrystallization. This paper describes factors that control grain refinement and superplastic forming characteristics of 6013. The effects of precipitate characteristics, cold rolling, and heat treatment temperatures on the recrystallization and grain refinement are discussed.

Introduction

A fine grain structure and its stability during high temperature deformation are the main requirements for superplastic forming. A study of the grain refining and superplastic forming of aluminum alloy 6013 is in progress.

The recrystallization process for obtaining a fine grain structure has been reviewed by many authors [1-3]. Wert [1] points out that the number density of large particles which produce deformation zones during mechanical processing is the most important factor for grain refining. Therefore, in order to produce a fine grain structure, the control of large constituent particles, large incoherent precipitates, and medium-size dispersoids is necessary. Precipitate phases in 6013 include the large constituent α(AlFeMnSi) particles which are formed during solidification, α-dispersoids which precipitate during high temperature heat treatments [4] and the strengthening precipitates β'(Mg_2Si), θ'(Al_2Cu) and Q which precipitate during normal aging treatments. Humphreys [2] has reviewed the process of recrystallization in alloys containing second phase particles. The interrelationship between particle size, d, deformation zone size, r, and the critical grain size for continued growth, R_{cr}, is presented as

$$r + 0.5d > R_{cr} = 2\gamma_s / \tau\rho_{matrix} \qquad (1)$$

where γ_s is the surface energy of the grain boundary, τ is the dislocation line tension, and ρ_{matrix} is the dislocation density in the matrix phase far from the precipitates [3].

In this model, the deformed zone near the precipitates is considered a well-defined, discontinuous area of the matrix phase. On the other hand, if it has structural continuity with the matrix phase, the area available to nucleate recrystallization can be changed. The size of this area may be obtained by analyzing the profile of the dislocation density near the precipitates.

The difference between these two models is apparent from the schematic diagrams shown in Fig. 1(a) and (b). If the deformation zone is discontinuous from the matrix phase, the dislocation density near the precipitates is as shown in Fig. 1(a). The size of the nucleus of the recrystallized grain is related only to the size of the deformation zone; it is independent of recrystallization

temperatures. The temperature change may affect R_{cr} by changing the surface energy of the grain boundary. As a result, survival of the recrystallized grain is critically dependent on the size of the deformed zone rather than on the heat-treating temperature.
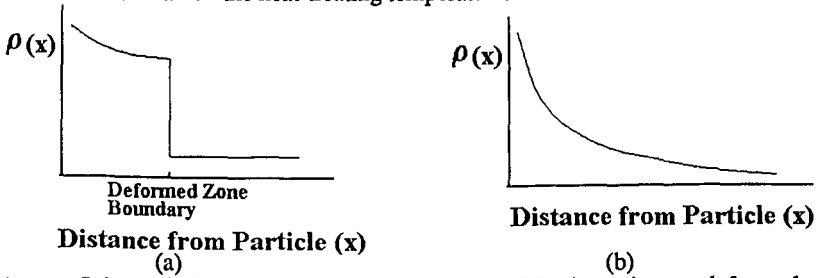

Figure 1.   Schematic illustration of deformed zone: (a) Discontinuous deformed zone; and (b) Continuous deformed zone.

On the other hand, if the deformation zone has continuity with the matrix phase, the dislocation density near the precipitates will be as shown in Fig. 1(b). The nucleus of the recrystallized grain is related to the profile of the dislocation density, $\rho^G(x)$, near the precipitates. The survival of newly produced grains is directly affected by the heat treating temperature. The critical density of dislocations for recrystallization, ρ^G*, is changed by the recrystallization temperature. The radius of the nucleation zone is determined by this ρ^G* level. The survival of recrystallized grains can be predicted by comparing the radius of the nucleation zone with R_{cr}.

Although it is difficult to obtain the exact value of ρ^G*, it is possible to assume ρ^G* relatively. By taking $\rho_{G_1}* > \rho_{G_2}*$ where the recrystallization temperature, T_2, is higher than T_1, we can compare and explain the size change of recrystallized grains in a qualitative sense at various aging, cold-rolling, and recrystallization temperatures.

The superplasticity of alloy 6013 has been tested in dynamic recrystallization conditions. The maximum elongation is 230%, and the true stress is 6.7 MPa at 521°C and 3×10^{-4}/sec strain rate conditions. To improve elongation, the amount of large inclusions, which seem to be a source of early cracks and high deformation stresses, should be reduced.

<u>Experimental Procedure</u>

Commercial 6013-T6 aluminum alloy sheet was used as the starting material; the chemical composition is shown in Table 1. All specimens were 10% cold rolled and overaged to obtain a uniform distribution of large precipitates. Overaging temperatures were from 270°C to 443°C. Overaged specimens were 60% to 80% cold rolled again and recrystallized at 400°C or 443°C for 40 min. Detailed overaging and recrystallizing conditions are given in Table 2. All specimens were heat treated in a salt-bath furnace for rapid heating, and the inclusions, precipitates, and grains were observed by optical and electron microscopes. The following parameters have been determined:

(1) Mean grain size (d): Grain sizes have been measured on the optical microstructure photographs by the line intercept method of Abram's procedure   (ASTM-E112) and described by the mean intercept distances of grain boundaries.

(2) Inter-particle spacing (λ_G):   Used as NL^{-1}. The number of particles in the unit length, NL^{-1}, has been obtained by the line intercept method. The NL^{-1} of large inclusions and rod-type precipitates has been measured separately. Since the NL^{-1} of large inclusions should be the same for all specimens, it was taken as the average value of NL^{-1}. Total NL^{-1} has been obtained by combining the NL^{-1} of rod-type precipitates to the averaged NL^{-1} of inclusions.

(3) Particle volume fractions (fv): These have been measured by a point counting method. Volume fractions of large inclusions and rod-type precipitates were measured separately. Total fv has been obtained by adding the volume fraction of large inclusions to that of rod-type precipitates.

Table 1. Chemical Composition of Aluminum Alloy 6013

Alloying Element	Mg	Si	Cu	Mn	Fe	Ti	Zr
Composition (w/o)	0.89	0.74	0.90	0.33	0.26	0.01	0.03

Superplasticity of the alloy was tested using warm-rolled specimens for dynamic recrystallization. Dynamically recrystallized specimens were made by aging at 380°C for 17 hours and warm rolling to 90% reduction at 195°C. The warm-rolled sheet was directly used for test specimens.

Formability has been tested using a high-temperature tensile test under constant cross-head speed. Stress, strain, and strain-rates have been calculated under the assumption of uniform deformation, and strain rate sensitivity, m, has been tested using a step strain-rate method [5]. For testing a specimen of only 0.3 mm thickness, supporting blocks on the specimen grip zone have been used.

Results and Discussion

Figure 2 shows large constituent particles in the 6013-T6 alloy sheet. These particles have been confirmed by EDS analysis as an α(AlFeMnSi) phase. The constituent particles are very stable; it was difficult to change their shape or size by heat treatment [4].
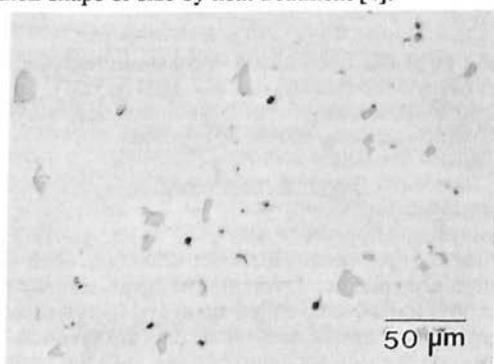

50 µm

Figure 2.   Large constituent particles observed in the 6013-T6 alloy. As-polished condition.

A typical microstructure observed in overaged specimens is shown in Fig. 3. The rod-type precipitates are newly developed β(Mg₂Si) by overaging. The size and distribution of these new precipitates are changed by overaging conditions. Uniform distribution of the new precipitates was obtained by 10% cold rolling before aging.

Figure 4 shows recrystallized grains. Fine grains occur for an aging temperature between 360-380°C. The resulting grain sizes are given in Table 2. Figure 5 shows the size of the recrystallized grains vs. aging temperature. The interesting feature of these curves is that all of the curves show a minimum grain size at about the same aging temperature. This indicates that there is

436

some optimum condition in the aging step for grain refining and that overaged precipitates play an important role in grain refining.
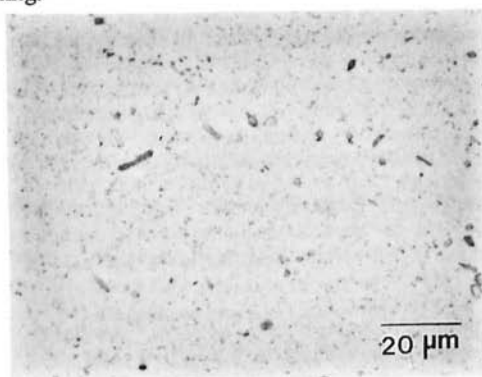

Figure 3.   Rod-type precipitates typically observed in overaged specimens. Etched by Keller's reagent.

Table 2. Heat-Treatment Conditions and Resulting Grain Sizes

| Aging Conditions		Particle Mean Free Path (μm) λ_G			Grain Size after Recrystallization (μm)			
					80% cold rolling/ recrystallized at		60% cold rolling/ recrystallized at	
Temp (°C)	Time (hr)	Inclusions	Precipitates	Combined	443°C	400°C	443°C	400°C
270	4.5	-	-	-	26.0	24.0	27.0	25.5
362	16.0	222	53.3	41.8	15.6	15.5	18.0	23.0
380	17.5	222	37.3	33.1	15.0	12.5	16.5	20.0
400	17.5	222	48.3	38.5	15.2	15.0	-	-
443	17.5	222	69.5	51.6	18.5	27.5	22.5	33.0

(a)   (b)
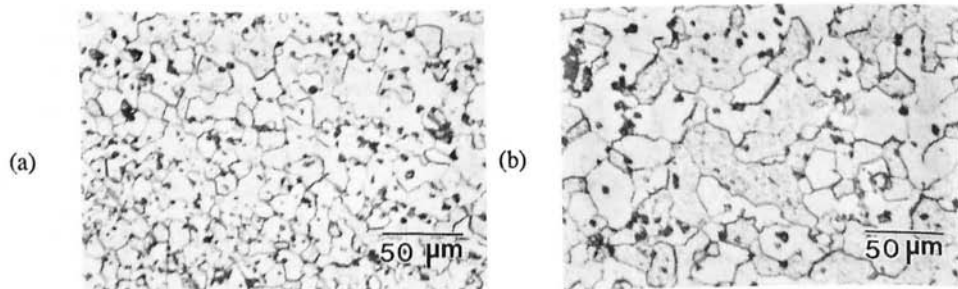
Figure 4.   Comparison of recrystallized grains in various heat-treatment conditions: (a) aged at 380°C and recrystallized at 400°C for 40 min.; and (b) aged at 443°C and recrystallized at 443°C for 40 min.

The recrystallized grains at 443°C do not show large differences due to a change in the amount of cold rolling. However, as shown in Fig. 5, those at 400°C are sensitive to the cold-rolling amount. The deformation zone model cannot explain the combined effects of cold rolling and recrystallization temperature on the grain size. In this model, the dislocation density changes abruptly at the end of the deformation zone. Therefore, the size of the nucleation zone (i.e., deformation zone) is not changed by the recrystallization temperature. The change of recrystallization temperature only affects R_α by changing the dislocation line tension, τ. Therefore, the effect of a change of recrystallization temperatures on the grain size should show the same trend at each aging temperature. This prediction does not meet with the experimental results.
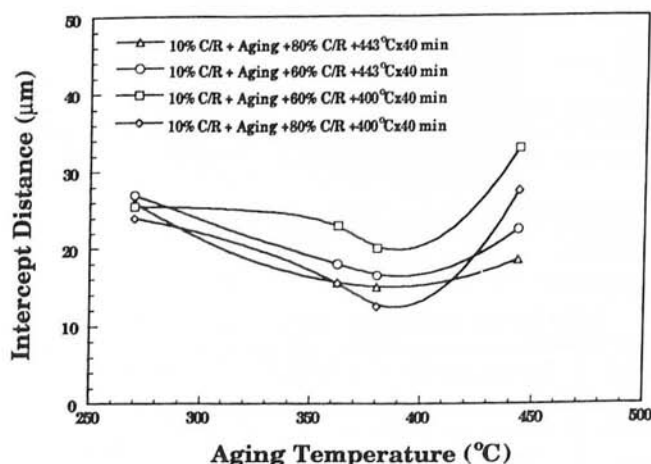

Figure 5.   The size of recrystallized grains vs. aging temperatures.

On the other hand, if the deformation area is continuous with the matrix phase, the dislocation density will change continuously. When a particle-containing alloy, e.g., dispersion-hardened materials, is deformed, severe deformation is generated near the particles. Dislocation density, increased by the shear deformation of dispersion-hardened materials, is described by Ashby [6], using

$$\rho^G = 1/\lambda_G \times 4\gamma/b \tag{2}$$

where λ_G is the geometric slip distance, γ is the shear strain, b is the Burger's vector, and ρ^G is the average dislocation density. Assuming that the deformation near hard particles is only related to the change of dislocation density and that the active site for nucleation is only determined by the level of the dislocation density, Equation (2) can be used to describe the recrystallization process. Equation (3) can be obtained by modifying Equation (2) to account for the change of the dislocation density near the precipitates:

$$\rho^G(x) = F(x)\ 1/\lambda_G \times\ 4\gamma/b \tag{3}$$

where x is the distance from a hard particle and $\rho^G(x)$ is the dislocation density at x. F(x) is a distribution function of dislocations which is influenced by the particle size, d; F(x) is assumed to be a function of the misorientation angle, θ. The dislocation density, ρ, is then approximated using θ^3. By empirical equation, [7]

$$\tan \theta\ =\ \tan \theta_{max}\ (\exp(-1.8x/2d)). \quad [7]$$

438

Then, $F(x) = A [\tan^{-1}\{ \tan\theta_{max} \exp(-1.8x/2d)\}]^3$ (4)

where A is a constant.

In this model, the size of the nucleation zone is changed by the recrystallization temperature. The nucleation zones at various conditions can be schematically illustrated (Fig. 6) by using Equation (3). In this diagram, if the recrystallization temperature, T_1, increases to T_2, the corresponding minimum dislocation density for recrystallization, $\rho G_1{}^*$, decreases to $\rho G_2{}^*$, and $(x/d)_1$ increases to $(x/d)_2$. In order to satisfy Equation (1) at these temperatures, the minimum size of the precipitates, d_1, must be larger then d_2. As only the precipitates larger than d_1 will actually take part in recrystallization at T_1, large (x/d) is more favorable to grain refining. Since the total number of precipitates is constant at a given aging condition, the number of precipitates contributing to recrystallization in the higher recrystallization temperature will be larger than those contributing at the lower recrystallization temperature.

If we assume the level of $\rho G_1{}^*$ and $\rho G_2{}^*$ relative to each other, we can explain the grain size changes in Fig. 5 by using Fig. 6. One way of doing this is by substituting in Equation (4) the particle size, d, for each heat-treated specimen, and then plotting $\rho^G(x)$ vs. x, Fig. 6(b). The particle size is obtained by averaging the diameter of large inclusions and the length of rod-type precipitates. In the specimen aged at 443°C, the number of precipitates contributing to the recrystallization at 443°C is larger than that at 400°C, and, therefore, the size of the recrystallized grains at 443°C is smaller than those at 400°C.

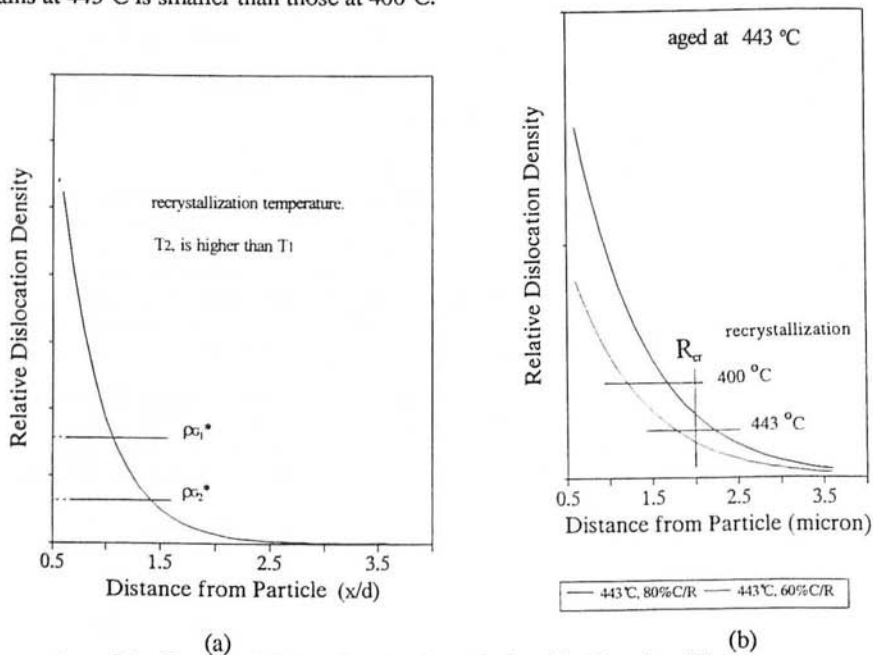|	
(a)	(b)

Figure 6.   Distribution of dislocation density calculated by Equation (3).

The dislocation-density curves for the specimens aged at 362°C and 380°C are almost the same as shown in Fig. 6(b), except that the curves are slightly shifted to the right. Among the 362°C and 380°C aged specimens, there is no large difference in the grain size between the 400°C and 443°C recrystallization temperatures for the 80% cold-rolled specimens. This may be due to the fact that the ρ^G curves of the 80% cold-rolled specimens are so steep that the critical distances of x at these

two recrystallization temperatures are almost the same. It may also be possible that the critical values of x at these two recrystallization temperatures are so large that almost all of the precipitates are taking part in the recrystallization process.

Figure 7 illustrates the change of grain size versus $1/\lambda_G$. The grain size is almost linearly proportional to the inverse of the inter-particle distance, $1/\lambda_G$, as described by Equation (2). The effect of the recrystallization temperature and cold deformation on grain size is also explained by Equation (3). The complicated behavior of the recrystallization reaction at various conditions is explained by Equation (3) and Fig. 6.
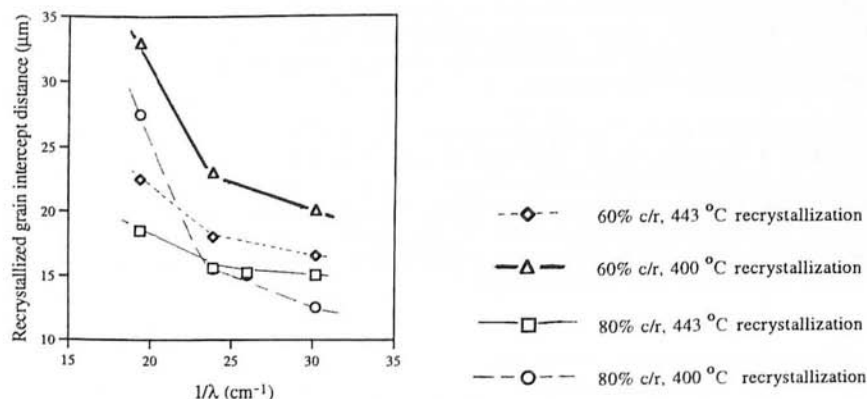

Figure 7.   The change of grain size vs. $1/\lambda_G$.

The superplasticity of this alloy is tested in dynamic recrystallization conditions. Even though the starting grain structure of the dynamically recrystallized specimen has not been observed, the microstructure observed after testing shows that it has a fine grain structure. The maximum elongation is 230%, and the deformation stress is 6.7 MPa at 521°C and 3×10^{-4}/sec strain rate conditions. The elongation is too small and the stress level is too high to compare with those of aluminum alloy 7475 [3]. To improve the elongation, the amount of large inclusions, which seem to be a source of early cracks and high deformation stresses, should be reduced.

Figure 8 shows the deformation stresses at various strain rates and temperatures. The change of strain rate sensitivity, m, can be derived from the slopes of the curves. The maximum m, 0.376, is obtained at 563°C and 3×10^{-4}/sec - 6×10^{-4}/sec strain rate range. The maximum m and the range of strain rate where the maximum m is obtained are similar to those of aluminum alloy 7475 [8].

The microstructure observed after high-temperature tensile tests contains small equiaxed grains and relatively large pores, some of which possess a slightly elongated shape. Figure 9 shows a microstructure typical of superplastically deformed materials. The elongated grain structure indicates that there is some slip deformation during the tensile test [9]. The deformation mode may be improved by reducing the grain size, lowering the strain rate, or testing at a slightly higher temperature [10].

Conclusions

A fine grain structure and its control are the main requirements for superplastic forming. A grain size about 12 mm in diameter was obtained in aluminum alloy 6013 by a recrystallization method. The recrystallization behavior in the alloy with large particles has been analyzed. A smooth change of deformation in the matrix near a large particle is proposed. The deformation amount is assumed

to be described by the change of the dislocation density. The effects of various aging temperatures, recrystallization temperatures, and degree of cold rolling on grain size are qualitatively explained by this model.
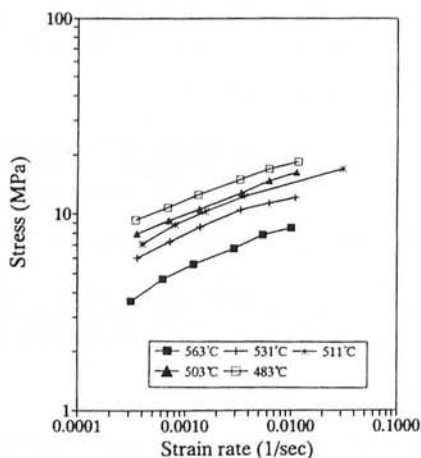

Figure 8.   Deformation stress at various strain rates and temperatures.
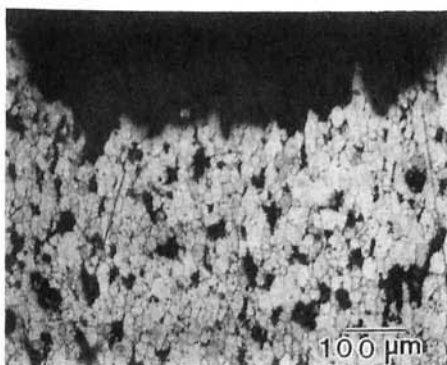

Figure 9.   Microstructure observed after high-temperature tensile test.   Etched by Keller's reagent.

Characterization of superplastic forming in commercial alloy 6013 is in progress. The nature of the deformation at 521°C and 3 x 10^{-4}/sec strain rate is grain boundary sliding, even though some minor contribution of slip deformation is also observed. The maximum elongation is 230%; the true stress is 6.7 MPa at 521°C and 3 x 10^{-4}/sec strain rate conditions. To improve elongation, the amount of large inclusions should be reduced. These inclusions seem to be a source of early cracks and high deformation stresses.

441

References

1. J.A. Wert, Superplastic Forming of Structural Alloys, ed. N.E. Paton and C.H. Hamilton (Warrendale PA: Proc. Inter. Symp. on Superplasticity and Utilization of Superplasticity in the Forming of Structures, San Diego, CA, June 1982), 69.

2. F.J. Humpreys, Acta Metall. 25 (1977), 1323.

3. R. Sandstroem, Recrystallization and Grain Growth of Multi-Phase and Particles Containing Materials, ed. N. Hansen, A.R. Jones, and T. Leffers (Proc. International Symp. on Met. and Mat Scie., Roskilde, Denmark, September 1980), 45.

4. R.A. Jeniski, Jr., B. Thanaboomsombut, and T.H. Sanders (1994), to be published.

5. A.K. Ghosh, Superplastic Forming of Structural Alloys, ed. N.E. Paton and C.H. Hamilton (Warrendale, PA: Proc. Inter. Symp. on Superplasticity and Utilization of Superplasticity in the Forming of Structures, San Diego, CA, June 1982), 85.

6. M.F. Ashby, Phil. Mag. 21 (1970), 399.

7. F.J. Humpreys, Recrystallization and Grain Growth of Multi-Phase and Particles Containing Materials, ed. N. Hansen, A.R. Jones, and T. Leffers (Proc. International Symp. on Met. and Mat Scie., Roskilde, Denmark, September 1980), 35.

8. C.H. Hamilton, C.C. Bampton and N.E. Paton, Superplastic Forming of Structural Alloys, ed. N.E. Paton and C.H. Hamilton (Warrendale, PA: Proc. Inter. Symp. on Superplasticity and Utilization of Superplasticity in the Forming of Structures, San Diego, CA, June 1982), 173.

9. T.G. Langdon, Superplastic Forming of Structural Alloys, ed. N.E. Paton and C.H. Hamilton (Warrendale PA: Proc. Inter. Symp. on Superplasticity and Utilization of Superplasticity in the Forming of Structures, San Diego, CA, June 1982), 27.

10. N. Ridley and J. Pilling, Superplasticity, ed. B. Baudelet and M. Suery (Inter. Conf. on Superplasticity, Grenoble, France, September 1985), 8-1.